

# Interparticle Potential and Sedimentation Behavior of Cement Suspensions: Effects of Admixtures

Christopher M. Neubauer,\* Ming Yang,\* and Hamlin M. Jennings\*†

Departments of \*Materials Science and †Civil Engineering, Northwestern University, Evanston, Illinois, USA

*DLVO theory has been applied to cement suspensions containing admixtures. Two different batches of the same cement, different only in storage history, are compared. It is found that, although their general sedimentation behavior is similar, differences exist in the zeta potential and basic chemistry. Both the superplasticizer and water-reducing admixture result in all cases in a stable dispersion, contrary to the theoretical prediction that only a coagulated suspension should exist. This finding suggests that steric hindrance plays a larger role compared to electric repulsion in the deflocculation of cement pastes than previously believed. Zeta potential and sedimentation data for  $\text{CaCl}_2$  and sugar are also presented. ADVANCED CEMENT BASED MATERIALS 1998, 8, 17–27. © 1998 Elsevier Science Ltd.*

**KEY WORDS:** Cement, Chemical admixtures, Rheology, Sedimentation

**A**dmixtures provide a very important method of controlling the behavior of cement based materials. They can be divided into several basic categories:

1. *Water reducers and superplasticizers* improve the flow of liquid paste. This reduces the amount of water required in the mix and leads to lower overall porosity.
2. *Retarders and accelerators* change the time to set and rate of reaction of cement.
3. *Air entraining agents* incorporate air in the paste to enhance freeze-thaw resistance.
4. *Shrinkage reducing admixtures* control dimensional stability.

The detailed mechanisms of water reducers, superplasticizers, accelerators, and retarders have not yet been

identified. This article focuses on the first two types of admixture listed.

Superplasticizers and water reducers generally improve the flow of liquid cement paste by changing the degree of flocculation in the system [1]. It is believed that these materials are adsorbed at the solid-liquid interface and alter the degree of flocculation in one of three ways [1,2]: (1) increasing the zeta potential of the material, causing larger repulsive forces between particles; (2) increasing solid-liquid affinity; or (3) steric hindrance, the introduction of physical barriers to flocculation. Previous research has shed some light on the relative importance of these mechanisms.

Ernsberger and France [3] showed that the addition of calcium lignosulfonates to cement paste disperses the cement particles and causes them to develop a negative zeta potential. Daimon and Roy [2,4] showed that when superplasticizers were added at concentrations up to 2% (by weight of cement), the zeta potential of these materials became increasingly negative, eventually reaching values between  $-30$  and  $-40$  mV. Similar results have been gathered by Andersen [5], who measured values between  $-20$  and  $-30$  mV for admixture concentrations up to 10% (by weight of cement), and by Andersen and coworkers [6], who measured values between  $-20$  and  $-35$  mV at concentrations up to 5% (by weight of cement). In contrast, the zeta potential of cement without admixtures is generally measured as being weakly negative up to  $-12$  to  $-15$  mV [5,7,8] due to  $\text{SiO}_2$  groups at the cement-grain interface [9], although Nagele [10] has reported positive values between 5 and 20 mV.

Daimon and Roy [2] have also shown that the water-cement affinity is unchanged or slightly decreased by the superplasticizers they studied, indicating that this is not a cause for dispersion, and that up to 1% of sulfonated naphthalene formaldehyde condensate (SNF) could be adsorbed onto the surface of cement grains. Banfill [11] stated that these data show multilayer adsorption up to 60 nm in thickness upon the cement grains, which suggests steric hindrance is

Address correspondence to: Dr. H.M. Jennings, Department of Civil Engineering and Materials Science and Engineering, Northwestern University, 2145 Sheridan Road, Evanston, Illinois 60208.

Received October 3, 1997; Accepted February 12, 1998.

equally important as a dispersing mechanism. This is supported by the work of Andersen [5] and Andersen and coworkers [6], which found that superplasticizers with higher molecular weights have an increased dispersing capability, although they attributed this result to a larger amount of electronegative charges per chain. More recently, Uchikawa and coworkers [12] have utilized an atomic force microscope to measure the interactive force between the surface of the cement clinker and an adsorbed admixture, and compared this with the zeta potential measured by the electrokinetic sonic amplitude method. They concluded that steric hindrance played an important role in the dispersion of cement pastes. However, most of the evidence points to the increase in zeta potential as the major mechanism for dispersion [1,4].

Far less is known about the activity of accelerators and retarders on the system. It has been shown that  $\text{CaCl}_2$ , a typical accelerator, increases the heat of hydration at early times, indicating that the hydration reaction is faster [10]. Other salts have been shown to act as accelerators, with a general trend that increasing charge and decreasing ion size will enhance the accelerating capacity of that material [10]. Retarders are believed to adsorb onto the surfaces of the cement particles and on early hydration products in favor of  $\text{Ca}^{2+}$  ions [10].

A recent article [13] reported the rheological properties of cement paste using sedimentation, zeta potential, and particle size analysis. DLVO theory (named after the four contributors: Derjaguin, Landau, Verwey, and Overbeek) was applied to cement systems to determine the state of flocculation for cement suspensions. Both experimental and theoretical work showed that the normal, neat cement suspensions were flocculated or coagulated, and that their high ionic strength in the aqueous phase should render the degree of flocculation insensitive to variations in zeta potential when it is between  $-20$  mV and  $20$  mV.

This article describes similar sedimentation experiments on a type I cement that was stored under two different sets of conditions. Although the original emphasis of this study was to investigate the effects of storage on cement behavior using a wide range of experimental techniques, it is possible to use a small subset of these experiments to help understand the role of chemical admixtures in the rheological behavior of cements. Specifically, the impact of superplasticizers, water-reducing admixtures, accelerators, and retarders was probed using sedimentation, zeta potential analysis, and particle size analysis in order to understand the influence of zeta potential on the rheological behavior.

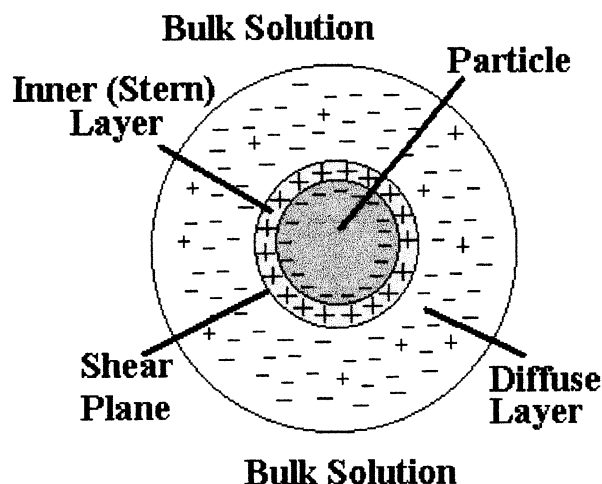


FIGURE 1. Electrical double layer model.

## Review of DLVO Theory

A brief review of pertinent DLVO theory will now be presented. For a more complete description, the reader is referred to Yang et al. [13].

A colloid suspension is typically defined as a suspension of particles smaller than  $10\ \mu\text{m}$  [14,15]. Most colloid suspensions consist of particles with charged surfaces [15-17]. These charges can be either intrinsic or can result from interactions between two phases through dissolution, adsorption, or ionization of interfacial surface groups. The electrostatic field that arises from these charges is described by the double layer model [15,16] as shown in Figure 1. The *inner*, or *Stern* layer, consists of counterions that are immobilized by the particles' surface.

Outside of the Stern layer region lies the *diffuse* layer, which is made up of ions that are repelled from the particle's surface due to the same sign charge. The boundary between the inner and diffuse layers is called the *shear plane*. The repelled ions in the diffuse layer give rise to an electrical potential that begins at the shear plane and decays with distance according to (see eq 1):

$$\psi = \psi_d \exp[-\kappa(r - a)] \quad (1)$$

where  $\psi_d$  is the electrical potential at the shear plane, also known as the zeta potential,  $\zeta$ ;  $\kappa$  is the Debye-Huckel parameter;  $r$  is the radial distance outward from the center of the particle; and  $a$  is the particle radius.

The thickness of the diffuse layer is defined by  $1/\kappa$  and can be approximated in water at  $25^\circ\text{C}$  by [13] (see eq 2):

$$\kappa(\text{nm}^{-1}) = 3.288 \sqrt{I_c} \quad (2)$$

where  $I_c$  is the ionic strength of the bulk solution (in moles/L), which for the cement concentrations described in this paper was calculated using eq 3:

$$I_c = \frac{1}{2} (C_{Na^+} + C_{K^+} + 4C_{Ca^{+2}} + C_{OH^-} + 4C_{SO_4^{2-}}) \quad (3)$$

where the concentration of  $OH^-$  was computed using the charge balance relation (see eq 4):

$$C_{Na^+} + C_{K^+} + 2C_{Ca^{+2}} = C_{OH^-} + 2C_{SO_4^{2-}} \quad (4)$$

as was done by Yang and coworkers [13]. The diffuse double layer in highly ionic systems such as cement is usually greatly compressed and typically only nanometers thick [18].

The surface charges result in a repulsive potential between particles described by (see eq 5):

$$U_R = 2\pi\epsilon_0\epsilon_r a \zeta^2 \ln\{1 + \exp[-\kappa(r - 2a)]\} \quad (5)$$

where  $\epsilon_0$  is the dielectric permittivity of free space and  $\epsilon_r$  is the relative dielectric constant of the liquid medium. This potential competes against an attractive force resulting from London-van der Waals forces given by [16] (see eq 6):

$$U_A = -\frac{A_H}{12} \left[ \frac{4a^2}{r^2 - 4a^2} + \frac{4a^2}{r^2} + 2\ln\left(1 - \frac{4a^2}{r^2}\right) \right] \quad (6)$$

where  $A_H$  is the Hamaker constant, which is sensitive to the type of material and the liquid medium.

DLVO theory accounts for the total interparticle potential through:

$$U_{tot} = U_R + U_A \quad (7)$$

where the attractive force is taken as negative. Since the attractive force is proportional to  $1/r^2$ , it is exerted over a much greater distance than the repulsive force, which falls off as  $\exp[-\kappa(r - 2a)]$ . Thus, the distance between surfaces within which the repulsive force is significant is given by the diffuse layer thickness,  $1/\kappa$ .

Using eq 7 and varying the overall ionic concentration while holding zeta potential and particle size constant produces the three types of curves shown in Figure 2. Curve A occurs at low ionic strength and high surface potential and represents a stable dispersion in which the particles repel each other. The larger the primary maximum,  $\psi_{max}$ , the more stable the dispersion. Curve B represents a flocculated suspension in which particles achieve an equilibrium separation,  $r_m$ , dictated by the secondary minimum,  $\psi_{sec}$ . This occurs in systems of moderate ionic concentrations. As the ionic

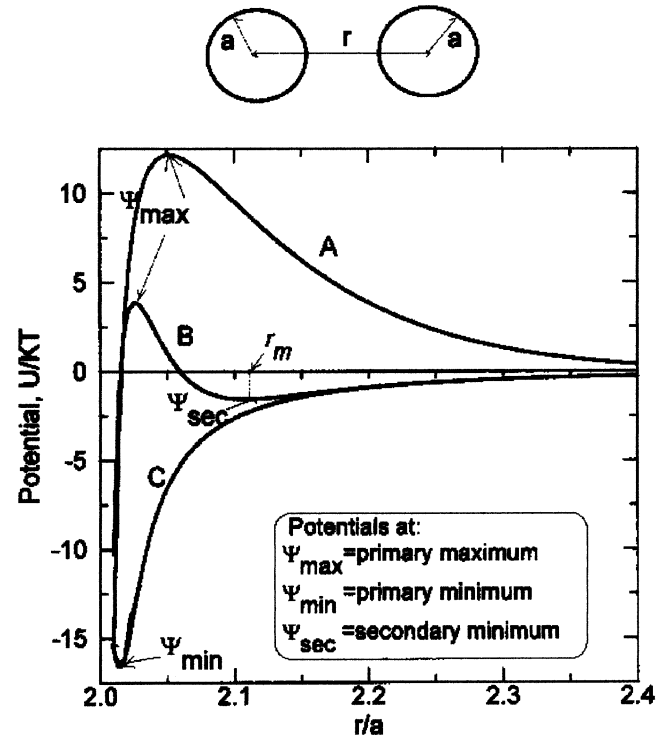


**FIGURE 2.** Illustration of interparticle potentials: (A) stable dispersion, (B) flocculated suspension, and (C) coagulated suspension.

strength increases, it will eventually reach a critical value and  $\psi_{max}$  will disappear, resulting in a coagulated suspension, shown in curve C. This critical concentration is given by [16] (see eq 8):

$$n_c = 3.648 \times 10^{-35} \frac{\zeta^2}{z^2 A_H^2} \quad (8)$$

where  $A_H$ ,  $\zeta$ , and  $n_c$  are in joules, volts, and moles/L, respectively. As long as the ionic concentration of the electrolyte is greater than the critical concentration, the interparticle potential, and therefore the state of flocculation, does not depend on ionic concentration. Table 1 gives the critical concentrations for coagulation using

**TABLE 1.** Theoretical critical concentration,  $n_c$  (mM), with  $A_H = 2.23 \times 10^{-20}$  J and  $z = 1$  for normal Portland cement

$ \zeta $ (mV)	Calculated $n_c$ (mM/L)
30	59.4
20	11.7
15	3.71
10	.0734
5	.0046
2	.0012

**TABLE 2.** Characterization of type I Portland cement

Oxide Composition			
CaO	63.22%	SO <sub>3</sub>	2.70%
SiO <sub>2</sub>	20.80%	MgO	4.15%
Al <sub>2</sub> O <sub>3</sub>	4.62%	Na <sub>2</sub> O	0.16%
Fe <sub>2</sub> O <sub>3</sub>	2.57%	K <sub>2</sub> O	0.51%
Bogue Composition			
C <sub>3</sub> S	54%	C <sub>3</sub> A	9%
C <sub>2</sub> S	19%	C <sub>4</sub> AF	8%
Blaine Fineness: 360 m <sup>2</sup> /kg			

normal cement systems with  $z = 1$  and  $A_H = 2.23 \times 10^{-20}$  J, the value for calcite as given in Russell et al. [15].

The sedimentation behavior of each system can be directly related to these three curves. Sedimentation,  $(H-h)/H$ , is defined by Yang and coworkers [13], where  $H$  is the initial height of the suspension, and  $h$  is the height of the sediment. A stable dispersion will exhibit free sedimentation behavior in which larger particles settle out first. A dark boundary is observed rising from the bottom to the top of the container as these larger particles settle, as noted by Yang et al. [13]. The water above the sediment is foggy as a result of the Brownian motion of the smallest particles. A particle size gradient forms between the top and bottom of the sediment. In stable dispersions,  $h$  is defined as the position of the dark boundary layer. Flocculated or coagulated suspensions will settle as flocs. If these flocs are large, the particles will settle rapidly. In this case, a boundary is observed at the top of the sediment, above which the water is clear as all of the particles will be incorporated into flocs. For flocculated or coagulated suspensions,  $h$  is defined as the boundary between the sediment and the clear water.

Chatterji [19] has suggested that the existence of a band of clear bleed water above the sediment column does not imply a flocculated sediment. He uses as an example a fully dispersed paste of Al<sub>2</sub>O<sub>3</sub>, which will also yield a band of clear bleed water above the sediment column. In fact, most sediments should produce a band of clear bleed water above the sediment column given enough time; the exception will be those that produce a rigid structure that prevents further settling of the particles. However, at early ages, the presence of clear bleed water above the sediment column is certainly suggestive of a flocculated paste where these tiny particles have been incorporated into the floc structure. Likewise, the presence of small particles in the water above the sediment column would be suggestive of a dispersed paste, where the particles can act more or less independently and are capable of Brownian motion, the random movement of tiny buoyant particles driven by thermal fluctuation.

Chatterji [19] has also suggested that artifacts may

result, since particles that appear to be flocculated will instead be a result of plaster of Paris set. In his earlier work, Chatterji [20,21] observed that pastes must be mixed repeatedly to remove any trace of plaster of Paris set. However, for particles to undergo plaster of Paris set, it is necessary that they exist in close proximity long enough for the hydration reaction to proceed; that is, they must be flocculated in solution or adjacent particles within the sedimented column. Therefore, plaster of Paris set should not affect observed results of particle behavior in the solution, as particles that undergo plaster of Paris set must already be in a flocculated state. It also will not affect observed sedimentation behavior at early ages. However, for the final sediment, plaster of Paris set must be considered as a possible mechanism, especially with respect to particle size.

## Experimental Method

A type I Portland cement was used in all cases to produce several different systems. Table 2 gives the composition and other data on this cement. Two different batches of this cement were used. Set I, labeled I hereafter, was stored indoors in a sealed condition for approximately 1.5 years. Set II, labeled O hereafter, was stored outdoors in an unsealed container (loose fitting top) for the same period of time. Batch O had noticeable chunks of cement that were difficult to break apart. In the experiments that follow, all of these chunks were broken before mixing. Batch I was fine and smooth, with no noticeable chunks.

Table 3 details the cement suspensions studied in this article. Each was made from 40 g of cement and 40 g of deionized (DI) water. The proper amount of admixture was combined with the mixing water and added to the cement. The suspensions were mixed by hand for 5 minutes and poured into 27-mm diameter plastic graduated cylinders. The sedimentation,  $(H-h)/H$ , as defined by Yang and coworkers [13], was recorded over time until no change was observed over 90 minutes.

After this time, a particle size analyzer using laser light scattering was used to measure the average particle size at the top and bottom of the sedimentation sample. A small amount of each sample was placed in the analyzer and sonicated for 30 seconds before analysis. The dispersion medium was DI water.

Zeta potential measurements were conducted using a Coulter Delsa 440, which uses electrophoretic light scattering principles to calculate the appropriate value. These samples were prepared by mixing a sample of the appropriate batch as described previously. After 30 minutes, aqueous solution was filtered using 0.1- $\mu$ m filter paper and a small amount of the unfiltered cement was re-dispersed. The ionic concentration of the re-



**TABLE 3.** Composition of cement suspensions

Batch ID	Cement Type	Admixture Information		
		Category	Type	Amount (weight %)
O1	O	Superplasticizer	Modified naphthalene sulfonate	0, 0.5, 1, 2, 3, 4, 5, 7
O2	O	Water reducer	Napthalene sulfonate, formaldehyde condensate	0, 0.5, 1, 2, 3, 4, 5, 7
O3	O	Accelerator	CaCl <sub>2</sub>	0, 0.5, 1, 2, 3, 4, 5, 7
O4	O	Retarder	Sugar	0, 0.5, 1, 2, 3, 4, 5, 7
I1	I	Superplasticizer	Modified naphthalene sulfonate	0, 1, 2, 5
I2	I	Water reducer	Napthalene sulfonate, formaldehyde condensate	0, 1, 2, 5

maining aqueous solution was determined using inductively coupled plasma (ICP) analysis.

## Results

### *Cements without Admixtures*

Both similarities and differences were found between the two batches of cement before any admixtures were added. Their sedimentation behavior was similar, with the particles in each separating from the top liquid at an initial height of ~50 mm to a final height of ~40 mm. This top liquid was clear and free of particles. Sedimentation of this type is characteristic of the flocculated or coagulated suspensions shown in curves B and C of Figure 2.

Particle size analysis indicates no size gradients along the vertical direction within the sediment for either cement, with Batch O having average particle sizes of 23.22 and 22.39  $\mu\text{m}$  and Batch I having average particle sizes of 20.67 and 19.86  $\mu\text{m}$  at the top and bottom of the sediments, respectively. This is also suggestive of a flocculated structure.

The zeta potentials of the two cements were very different. Batch O possessed an average zeta potential of  $-12.0$  mV, whereas Batch I possessed an average zeta potential of  $4.4$  mV. The negative value agrees extremely well with the values presented by several other authors [5,7,8], whereas the positive value agrees well with the values presented by Nagele [10]. ICP analysis of the basic chemistry of the two cement batches also shows significant changes, as shown in Table 4. The most significant difference is that Batch I has lower  $\text{SO}_4^{-2}$ ,  $\text{Na}^+$ , and  $\text{K}^+$  in solution than does Batch O. This suggests that the surface chemistry of the cement particles has been altered by exposure. However, comparison between Tables 4 and 1 at the appropriate zeta potentials shows that the ionic concentration of both pastes is an order of magnitude above the critical concentration for coagulation, so their basic sedimenta-

tion behavior should be, as is observed, similar. This is consistent with Yang et al. [13].

### *Effects of Superplasticizer*

**BATCH O1 (STORED OUTSIDE, SUPERPLASTICIZER).** The addition of superplasticizer greatly alters the sedimentation behavior. Beginning between 2% and 3% (by weight of cement) of superplasticizer, a dark area of sediment develops at the bottom of the graduated cylinder. The light and dark regions of this sediment are easily distinguishable, and the top of this dark region is recorded as the sedimentation height,  $h$ . This type of sedimentation behavior is a result of a stable dispersion, represented by curve A in Figure 2. The water above the sediment ranges from slightly to very foggy. Figure 3 depicts the sedimentation behavior of the O1 series, including the cross-over that occurs between 2 and 3 weight % superplasticizer.

Average particle size analysis confirms the presence of particle size differences between the top and bottom of the sample, as shown in Table 5. These data clearly show the altered sedimentation state that apparently begins at 1 weight % admixture, but becomes very apparent at 2 weight % admixture. However, as noted by Chatterji [19], it must be considered that the bottom of the sediment may have undergone a small amount of

**TABLE 4.** Inductively coupled plasma analysis of cement O and cement I

	Cement O	Cement I
$\text{SO}_4^{-2}$	26.3	11.2
$\text{Ca}^{+2}$	23.4	29.6
$\text{Na}^+$	12.8	2.0
$\text{K}^+$	64.8	3.8
$\text{OH}^-$	71.7	42.6
pH	12.85	12.63
$\text{I}_C$	174.2	105.8

Note: All concentrations are in mmol/L.

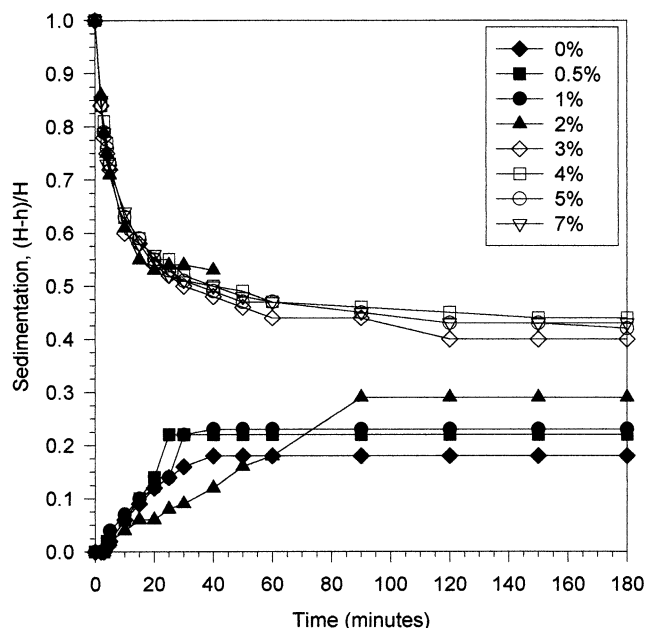


**FIGURE 3.** Sedimentation of Batch O1 with various amounts of admixture #1 (by weight of cement).

hydration, which may skew the data slightly. Both the sedimentation and particle size data are consistent with the change from a flocculated or coagulated state to a stable dispersion. As noted previously, this change must occur due to either increased zeta potential or steric hindrance.

Zeta potential measurements for Batch O1 are also shown in Table 5. The addition of superplasticizer causes the zeta potential to become increasingly negative, finally plateauing at approximately  $-30$  mV. These results correlate extremely well with the results of other researchers [2,4–6]. An increase in the magnitude of the zeta potential will cause the repulsive forces between particles to increase, driving them apart and causing a

stable dispersion. This is consistent with much of the data about the mechanisms of superplasticizers [1,4].

DLVO theory, however, suggests a mechanism other than zeta potential. Table 5 shows the results of ICP analysis on Batch O1. Comparison with Table 1 shows that these ionic concentrations remain at least  $2\times$ , and usually  $2.5\text{--}3\times$ , the critical concentration for coagulation. Thus, all of Batch O1 should be in a coagulated state that is insensitive to zeta potential fluctuations; this is clearly not the case. One scenario is that cement particles are physically separated by polymer molecules of the superplasticizer; thus, steric hindrance may play a large role in the deflocculation of cement paste by the superplasticizer, as suggested by Banfill [11]. This is also consistent with the work of Andersen [5], Andersen and coworkers [6], and Uchikawa et al. [12].

**BATCH I1 (STORED INSIDE, SUPERPLASTICIZER).** Batch I1 behaved very differently than Batch O1. First, as Figure 4 shows, the sedimentation is that of a flocculated or coagulated suspension at all concentrations of superplasticizer. A slight change in the sediment structure is suggested between 3% and 4% superplasticizer, but this is not reflected in any of the other data shown in Table 6. In all cases, the sedimentation is still indicative of a flocculated or coagulated system. Table 6 supports this data, as the ionic strength in all cases was well above the critical concentration for coagulation for all zeta potentials measured. Batch I1 behaves exactly as predicted by DLVO theory, and the addition of up to 7% (by weight of cement) superplasticizer does not affect its behavior in any way.

### Effects of Water-Reducing Admixture

**BATCH O2 (STORED OUTSIDE, WATER-REDUCING ADMIXTURE).** Figure 5 shows the sedimentation behavior of Batch O2. Table 7 shows the zeta potential, average particle size, and ICP analysis results. These results are very similar to those of Batch O1. Again, a cross-over from a

**TABLE 5.** Zeta potential, particle size analysis, and inductively coupled plasma (ICP) analysis for Batch O1

	Amount of Admixture 1 (by weight of cement)							
	0%	0.5%	1%	2%	3%	4%	5%	7%
Zeta potential (in mV)	−12.0	−5.4	−13.5	−28.0	−29.6	−26.3	−27.4	−23.7
Average particle size (in $\mu\text{m}$ )								
Top of sediment	23.22	18.11	13.69	7.60	11.04	11.12	4.50	9.54
Bottom of sediment	22.39	19.97	19.18	26.28	25.81	22.78	28.93	31.65
ICP analysis (in mmol/L)								
$\text{SO}_4^{2-}$	26.3	29.3	33.6	39.3	34.9	30.4	35.2	48.1
$\text{Ca}^{+2}$	23.4	22.7	24.0	25.2	23.1	18.5	22.9	26.0
$\text{Na}^+$	12.8	14.3	14.9	15.0	12.6	9.1	11.5	11.5
$\text{K}^+$	64.8	71.7	72.0	64.0	48.4	33.0	38.6	34.3
$\text{OH}^-$	71.8	72.7	67.7	50.9	34.7	18.4	25.5	1.5
pH	12.86	12.86	12.83	12.71	12.57	12.27	12.41	11.17
$I_c$	174.2	183.4	192.5	194.0	165.3	128.0	153.9	171.8

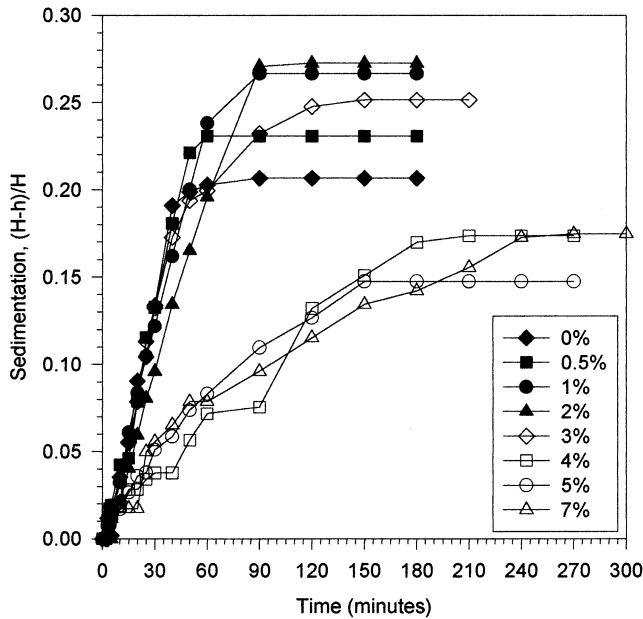


**FIGURE 4.** Sedimentation of Batch I1 with various amounts of admixture #1 (by weight of cement).

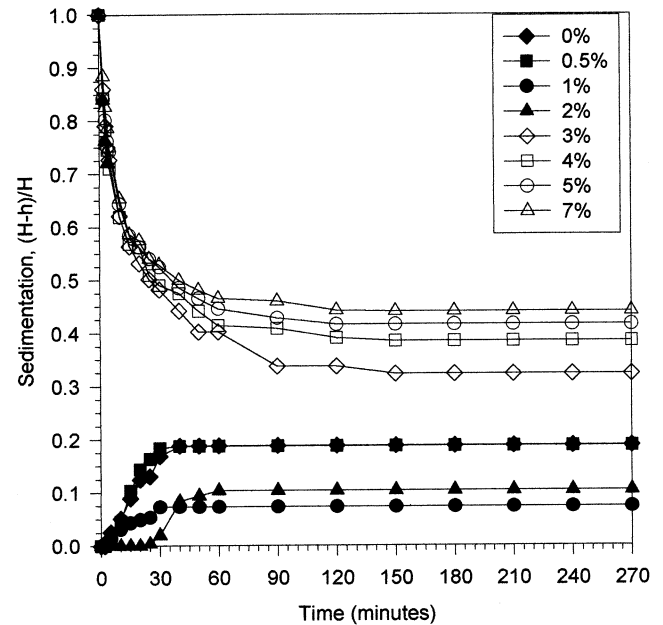


**FIGURE 5.** Sedimentation of Batch O2 with various amounts of admixture #2 (by weight of cement).

coagulated or flocculated suspension to a stable dispersion is noted between 2 and 3 weight % water-reducing admixture. Both the sedimentation and average particle size data reflect this change. The zeta potential results reach  $-27.6$  mV at 2 weight % admixture, but are typically around  $-20$  mV. This is consistent with the work cited previously. The ICP data again predict an ionic concentration approximately  $3\times$  that of the critical concentration. Therefore, steric hindrance must again play a role in the dispersion of cement particles in the presence of a water-reducing admixture.

**BATCH I2 (STORED INSIDE, WATER-REDUCING ADMIXTURE).** Batch I2 can be compared to Batch O2 in much the same way that Batch I1 compared to Batch O1. This batch behaved

as a coagulated or flocculated suspension over the entire range of admixture contents, as shown in Figure 6. At 5% and 7% admixture content, it is again observed that sedimentation becomes more difficult and the water above the sediment column becomes very cloudy as it is filled with small particles. The average particle size analysis shown in Table 8 also shows that a size difference develops at 7% admixture content. The zeta potential data show that the maximum zeta potential magnitude coincides with this phenomenon. It suggests that the flocculated/coagulated structure is unstable at these admixture concentrations and that the admixture is beginning to disperse the particles. However, the ICP data again show that the ionic concentration is well

**TABLE 6.** Zeta potential, particle size analysis, and inductively coupled plasma (ICP) analysis of Batch I1

	Amount of Admixture 1 (by weight of cement)							
	0%	0.5%	1%	2%	3%	4%	5%	7%
Zeta potential (in mV)	4.4		-2.6	-17.8			-13.1	
Average particle size (in $\mu\text{m}$ )								
Top of sediment	20.67	18.33	20.34	18.11	18.88	18.01	14.95	17.59
Bottom of sediment	19.86	19.07	18.85	16.85	19.24	19.85	16.68	18.29
ICP analysis (in mmol/L)								
$\text{SO}_4^{-2}$	11.2		14.0	16.1			18.1	
$\text{Ca}^{+2}$	29.6		31.1	30.4			29.3	
$\text{Na}^+$	2.0		3.2	4.4			7.3	
$\text{K}^+$	3.8		3.8	3.8			3.5	
$\text{OH}^-$	42.6		41.2	36.7			33.3	
pH	12.63		12.61	12.56			12.52	
$I_c$	105.8		114.4	115.4			116.8	

**TABLE 7.** Zeta potential, particle size analysis, and inductively coupled plasma (ICP) analysis of Batch O2

	Amount of Admixture 2 (by weight of cement)							
	0%	0.5%	1%	2%	3%	4%	5%	7%
Zeta potential (in mV)	−12.0	−23.0	−15.2	−27.6	−23.2	−18.2	−19.4	−19.9
Average particle size (in $\mu\text{m}$ )								
Top of sediment	23.22	16.07	17.87	9.71	3.11	5.34	6.26	5.76
Bottom of sediment	22.39	18.36	16.29	22.17	25.71	20.23	17.29	22.07
ICP analysis (in mmol/L)								
$\text{SO}_4^{2-}$	26.3	33.3	44.0	54.5	49.5	52.8	60.0	62.2
$\text{Ca}^{+2}$	23.4	23.2	26.7	28.7	27.0	25.7	26.9	25.7
$\text{Na}^+$	12.8	13.8	15.0	16.1	16.8	19.3	22.9	25.5
$\text{K}^+$	64.8	59.2	58.7	54.0	45.6	47.0	51.1	52.4
$\text{OH}^-$	71.8	52.7	39.1	18.3	17.3	12.2	7.7	4.8
pH	12.86	12.72	12.59	12.26	12.24	12.09	11.89	11.68
$\text{I}_C$	174.2	175.8	197.9	210.6	192.8	196.4	214.5	217.2

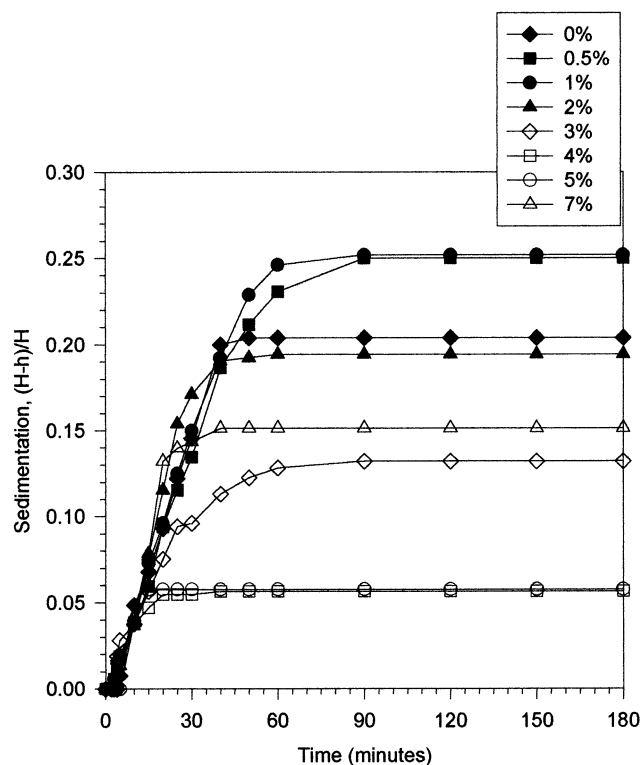
above the critical concentration for coagulation at all admixture concentrations; therefore, the stability of this sediment should be unaffected by variations in zeta potential  $<30$  mV. Thus, steric hindrance again is a likely source to account for the onset of dispersion.

### Effects of Accelerators and Retarders

**BATCH O3 (STORED OUTSIDE,  $\text{CaCl}_2$ ).** Figure 7 shows the sedimentation behavior of Batch O3. Table 9 shows the zeta potential, average particle size, and ICP analysis

results. All of the data are consistent with the sedimentation of a coagulated paste with the exception of the particle size measurements at 5% and 7%  $\text{CaCl}_2$ . However, these two points may be the result of hydration, as large particles settled to the bottom and became coated with early hydration product, undergoing the plaster of Paris set discussed by Chatterji [19]. This would be consistent with the known tendency of  $\text{CaCl}_2$  to accelerate the hydration reactions in cement based materials. The cross-over from negative to positive zeta potential (shown in Table 9) suggests that the calcium is satisfying the unresolved  $\text{SiO}_2$  groups present at the cement particle surface at higher concentrations of  $\text{CaCl}_2$ . The observed behavior is consistent with DLVO theory.

**BATCH O4 (STORED OUTSIDE, SUGAR).** The sedimentation of Batch O4 was similar to that of Batch O3, as shown in Figure 8. This batch also settled only as flocculated or coagulated suspension with no cross-over point to a stable dispersion. The average particle size analysis and ICP data shown in Table 10 support this finding. Table 10 also shows that the zeta potential of cement becomes increasingly less negative. The observed behavior again is consistent with DLVO theory.

**FIGURE 6.** Sedimentation of Batch I2 with various amounts of admixture #2 (by weight of cement).

## Discussion

For all of the suspensions analyzed, the ionic concentrations were well above the critical concentrations for coagulation at the zeta potentials measured. However, it is interesting to note that the cement stored outside was dispersed at higher concentrations of water-reducing admixture and superplasticizer, whereas the cement stored inside was not. As the chemical and zeta potential differences between the two cements are accounted for by DLVO theory, a physical reason for why steric hindrance is effective on one cement but not the other must be found. The answer appears to be the effective surface area of the cement.



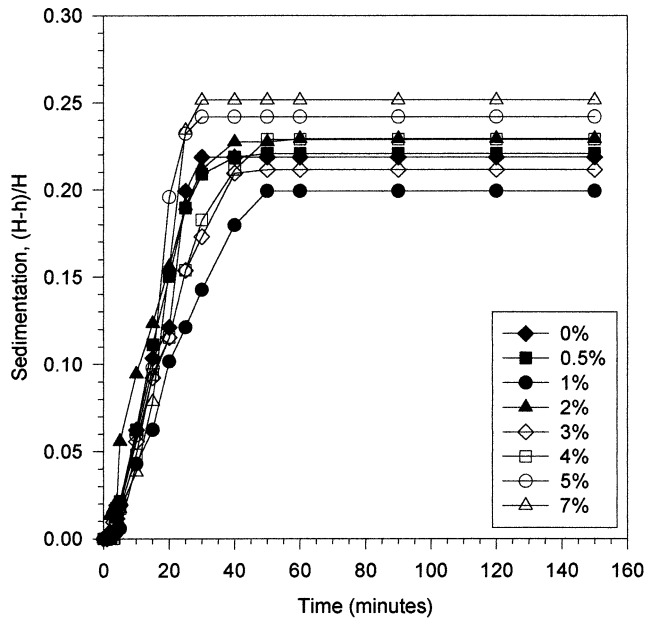


**FIGURE 7.** Sedimentation of Batch O3 with various amounts of admixture #3 (by weight of cement).

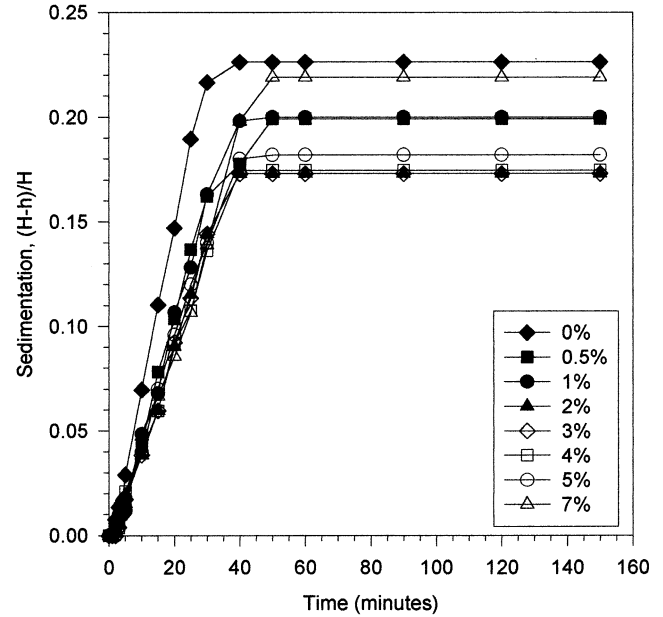


**FIGURE 8.** Sedimentation of Batch O4 with various amounts of admixture #4 (by weight of cement).

**TABLE 8.** Zeta potential, particle size analysis, and inductively coupled plasma (ICP) analysis of Batch I2

	Amount of Admixture 2 (by weight of cement)							
	0%	0.5%	1%	2%	3%	4%	5%	7%
Zeta potential (in mV)	4.4		−8.2	−9.5			−27.1	
Average particle size (in $\mu\text{m}$ )								
Top of sediment	20.67	17.65	16.89	16.99	16.15	17.95	15.56	13.64
Bottom of sediment	19.86	17.01	18.25	17.13	16.20	16.91	18.45	28.36
ICP analysis (in mmol/L)								
$\text{SO}_4^{-2}$	11.2		14.4	16.7			27.1	
$\text{Ca}^{+2}$	29.6		26.7	25.3			23.4	
$\text{Na}^+$	2.0		7.8	13.8			31.1	
$\text{K}^+$	3.8		10.5	16.9			36.8	
$\text{OH}^-$	42.6		42.9	48.0			60.6	
pH	12.63		12.63	12.68			12.78	
$\text{I}_C$	105.8		112.8	123.2			165.3	

**TABLE 9.** Zeta potential, particle size analysis, and inductively coupled plasma (ICP) analysis of Batch O3

	Amount of Admixture 3 (by weight of cement)							
	0%	0.5%	1%	2%	3%	4%	5%	7%
Zeta potential (in mV)	−12.0	−6.5	−4.6	5.2	23.3	8.5	3.2	7.2
Average particle size (in $\mu\text{m}$ )								
Top of sediment	23.22	20.75	21.73	22.15	23.23	28.00	22.28	22.31
Bottom of sediment	22.39	21.95	23.91	24.63	21.83	24.20	42.32	51.98
ICP analysis (in mmol/L)								
$\text{SO}_4^{-2}$	26.3	17.0	13.0	9.7	8.7	7.4	7.6	6.8
$\text{Ca}^{+2}$	23.4	28.6	32.2	35.6	35.9	36.1	36.1	35.4
$\text{Na}^+$	12.8	11.5	11.6	11.9	12.0	12.2	12.5	12.7
$\text{K}^+$	64.8	66.6	63.2	64.9	67.6	66.2	66.4	68.4
$\text{OH}^-$	71.8	101.2	113.4	128.6	134.0	135.9	135.9	138.2
pH	12.86	13.01	13.05	13.11	13.13	13.13	13.13	13.14
$\text{I}_C$	174.2	180.8	184.4	193.2	196.1	194.1	194.7	194.0

**TABLE 10.** Zeta potential, particle size analysis, and inductively coupled plasma (ICP) analysis of Batch O4

	Amount of Admixture 4 (by weight of cement)							
	0%	0.5%	1%	2%	3%	4%	5%	7%
Zeta potential (in mV)	−12.0	−10.9	−6.1	−5.7	−3.5	−2.6	−2.9	−3.2
Average particle size (in $\mu\text{m}$ )								
Top of sediment	23.22	20.80	20.16	18.53	21.26	18.08	18.81	18.05
Bottom of sediment	22.39	23.26	22.74	24.59	23.59	22.86	23.71	26.41
ICP analysis (in mmol/L)								
$\text{SO}_4^{2-}$	26.3	37.3	38.4	37.1	34.7	35.3	33.6	33.6
$\text{Ca}^{+2}$	23.4	27.8	28.9	31.4	32.4	33.4	34.2	35.3
$\text{Na}^+$	12.8	12.1	13.3	12.7	12.3	11.9	11.6	11.5
$\text{K}^+$	64.8	67.2	65.1	62.4	64.5	61.6	59.8	59.5
$\text{OH}^-$	71.8	60.3	59.3	63.7	72.2	69.8	72.5	74.5
pH	12.86	12.8	12.8	12.8	12.9	12.8	12.9	12.9
$\text{I}_C$	174.2	200.1	203.4	206.3	208.7	209.1	207.6	210.6

It was noted in the Experimental Method section that the cement stored outside was chunky and had to be broken before mixing, which indicates that some hydration had taken place. Also, as noted in the Results section for cements without admixtures, the cement that was stored outside possessed a particle size of 23.22  $\mu\text{m}$  at the top of the sediment and 22.39  $\mu\text{m}$  at the bottom of the sediment, compared with 20.67 and 19.86  $\mu\text{m}$  at the top and bottom of the sediment, respectively, for the cement stored inside. Thus, if one assumes roughly spherical particles (on average), the cement stored inside will have a higher surface area than the cement stored outside. This increased surface area can affect the ability of a polymer to cause steric hindrance in two ways.

First, the higher surface area will require more admixture to effectively coat the surface. Thus, the resulting layer on the surface of the cement particles may be too thin to cause steric hindrance, or it may result in incomplete coverage of the surface. In either case, the particles will still be able to flocculate.

Second, the increased surface area will result in a greater reactivity, which generates more hydration product. It is possible that some of the admixture will be incorporated into this hydration product and will be unavailable to participate in dispersing the system. Essentially, this situation reverts to the first case described previously, as the resulting layer may be too thin or too incomplete to prevent flocculation. In either case, it shows clearly that controlling the storage history may be an effective method to utilize admixtures more efficiently.

## Conclusions

The following conclusions can be drawn from this work:

1. The zeta potential and chemistry of a cement are influenced by its storage history. Both positive and negative zeta potentials are possible. This is consistent with the work in the literature. It may be possible to reduce the amount of admixtures required by controlling the storage history of the cement.
2. Steric hindrance may play a larger role in deflocculation than previously believed. This has been previously suggested by Banfill [11] and more recently by Uchikawa and coworkers [12]. DLVO theory predicts that cement paste suspensions should be stable to zeta potential variations <30 mV. Although none of the four admixtures created a zeta potential outside this range, significant differences were noted in the sedimentation behavior of these materials.
3. Superplasticizers and water-reducing admixtures both cause the zeta potential of cement pastes to become increasingly negative. This is consistent with the work of other authors [2,4–6].
4.  $\text{CaCl}_2$  causes the zeta potential of cement to become positive. Cement suspensions are stable in the presence of this admixture.
5. Sugar causes the zeta potential of cement to decrease in magnitude, but to remain negative. Again, cement suspensions are stable in the presence of sugar.

## Acknowledgments

This work was supported by the National Science Foundation's Science and Technology Center for Advanced Cement Based Materials. C.M.N. wishes to thank the Department of Defense for funding via a National Defense Science and Engineering Graduate Fellowship.

## References

1. Taylor, H.F.W., *Cement Chemistry*; Academic: London, 1990.
2. Daimon, M.; Roy, D.M. *Cem. Concr. Res.* **1978**, *8*, 753–764.
3. Ernsberger, F.M.; France, W.G. *Ind. Eng. Chem.* **1945**, *37*, 598–600.
4. Daimon, M.; Roy, D.M. *Cem. Concr. Res.* **1979**, *9*, 103–110.
5. Andersen, P.J. *Cem. Concr. Res.* **1986**, *16*, 931–940.
6. Andersen, P.J.; Roy, D.M.; Gaidis, J.M. *Cem. Concr. Res.* **1987**, *17*, 805–813.
7. Nagele, E. *Cem. Concr. Res.* **1986**, *16*, 853–863.
8. Zelwer, A. *Proc. 7th International Congress on the Chemistry of Cement* **1980**, *2*, II/147–II/152.
9. Muhua, T.; Roy, D.M. *Cem. Concr. Res.* **1987**, *17*, 983–994.
10. Nagele, E. *Cem. Concr. Res.* **1985**, *15*, 453–462.
11. Banfill, P.F.G. *Cem. Concr. Res.* **1979**, *9*, 795–796.
12. Uchikawa, H.; Hanehara, S.; Sawaki, D. *Cem. Concr. Res.* **1997**, *27*, 37–50.
13. Yang, M.; Neubauer, C.M.; Jennings, H.M. *Adv. Cem. Based Mater.* **1997**, *5*, 1–7.
14. Buscall, R.; White, L.R. *J. Chem. Soc. Lon. Far. Trans. 1* **1987**, *83*, 873–891.
15. Russell, W.B.; Saville, D.A.; Schowalter, W.R. *Colloidal Dispersions*; Cambridge University: Cambridge, 1989.
16. Hunter, R.J. *Foundations of Colloid Science, Volume 1*; Oxford University: New York, 1987.
17. Myer, D. *Surfaces, Interfaces, and Colloids: Principles and Applications*; VCH: New York, 1991.
18. Tattersall, G.H.; Banfill, P.F.G. *The Rheology of Fresh Concrete*; Pitman Advanced: London, 1983.
19. Chatterji, S. Personal Communication to Hamlin M. Jennings.
20. Chatterji, S. *Cem. Concr. Res.* **1986**, *16*, 967–970.
21. Chatterji, S. *Cem. Concr. Res.* **1988**, *18*, 615–620.